# Miscibility and Hydrogen Bonding in Blends of Poly(ethylene oxide) and Kraft Lignin

**John F. Kadla* and Satoshi Kubo**

*College of Natural Resources, North Carolina State University, Raleigh, North Carolina 27695-8005*

*Received June 19, 2003; Revised Manuscript Received July 15, 2003*

ABSTRACT: Polymer blending is a convenient method to develop products with desirable properties. Through specific intermolecular interactions favorable polymer blending can occur, and composite materials with desirable properties can be produced. In this study we have prepared poly(ethylene oxide)−lignin blends using thermal mixing. Miscible blends were observed over the entire blend ratio. A melting point depression, comparable to results obtained from phenoxy/PEO blends, and a negative deviation of $T_g$ from the weight-average values was observed. The effect of the binary interaction parameter, $\chi$, on $T_g$ was analyzed. Satisfactory prediction of the $T_g$−composition curve was obtained, in which specific intermolecular interactions exist. FT-IR analyses revealed a strong hydrogen bond between the aromatic hydroxyl proton and the ether oxygen in PEO.

## Introduction

Recently, there has been a rising interest in biomaterials utilizing natural polymers, owing to the low cost, biodegradability, and biocompatibility.[1] Polymer blending is of considerable importance as an alternative to graft copolymerization and the high cost to develop new homopolymers. Extensive research has been undertaken in blending different polymers to obtain new products having some of the desired properties of each component.[2−5]

Lignin, a natural polymer found in wood, is a polyaromatic polyol that is readily available and relatively inexpensive. Lignin structure is dependent on wood species and processing conditions.[6] Commercially, lignin is obtained as a byproduct of "wood free" papermaking. Some industrial processes consistently produce standard well-defined lignins. As a result, lignin is utilized as a stabilizer (antioxidant) for plastics and rubber as well as in the formulation of dispersants, adhesives and surfactants. Lignin has also been used in the production of fully biodegradable lignin grafted polyolefins.[7]

Extensive cross-linking and strong intramolecular interactions of polymeric lignins constrain the utilization of polymeric lignin in solid material systems.[6,8] Through polymer blending these interactions can be disrupted, thus altering the lignin's viscoelastic properties.[6] However, as with most polymeric systems, the observation of miscible polymer blends with lignin are rare.[9]

Polymer blending is a convenient method to develop products with desirable properties. The chemical and physical properties of the polymer blends are dependent on monomer type(s), molecular weight, and distribution and composition of the respective polymers. Most polymers however are immiscible due to the low entropy of mixing.[10] Only through specific intermolecular interactions can favorable polymer blending occur and composite materials with desirable properties be produced.

Various techniques exist to determine the miscibility of polymer blends,[11] including thermal analysis,[12] dynamic mechanical analysis,[13] microscopy,[14] and solid-state NMR.[15] Thermal analysis, specifically DSC can determine whether two or more polymers are miscible or immiscible. A single compositional-dependent glass transition temperature ($T_g$) is an indication of full miscibility at a dimensional scale between 5 and 15 nm.[11] On the basis of the composition of the blend, the $T_g$s of the individual components, and the nature of the interactions between these components, several theoretical and empirical equations have been proposed for the prediction of blend $T_g$.[16−23]

A powerful tool to detect specific intermolecular interactions in polymer blends is Fourier transform infrared (FT-IR) spectroscopy. Observed changes in hydroxyl, carbonyl and ether vibrations provide direct evidence of specific interactions between blend components.[12,24] The magnitude of the shift in wavenumber ($\Delta\nu$) arising due to blend formation yields a measure of the average strength of the intermolecular interactions.[25]

In this paper, the miscibility of lignin/poly(ethylene oxide) (PEO) blends of varying composition was measured by thermal analysis. The interaction parameter and energy density between blend components were estimated using melting point depression and glass transition temperature measurements. FT-IR spectroscopy was used to study the intermolecular interactions between lignin and PEO. Using lignin model compounds, the role of the aliphatic and phenolic hydroxyl groups in the interaction with PEO was determined.

## Experimental Section

**Materials.** Hardwood kraft lignin was obtained from Westvaco Corp. The lignin was repeatedly washed with dilute HCl (Aldrich Chemicals) to exchange sodium counterions, vacuum-dried over $P_2O_5$, and recovered as a fine powder. Chemical properties of the lignin are listed in Table 1. Poly(ethylene oxide) (PEO), 100 000 amu (Union Carbide Corp.) and polystyrene (PS), 140 000 amu (Aldrich Chemicals) were used as received. Sodium borohydride ($NaBH_4$), sodium hydroxide (NaOH), and all solvents were purchased from Aldrich Chemicals and used as received. Carbon tetrachloride used for FT-IR measurement was dried over 4A activated molecular sieves before use. 3,4-Dimethoxy acetophenone, 2-methoxy-4-hydroxyphenol, 3-(3,4-dimethoxy phenyl)-1-propanol (**I**), 2-meth-

* Corresponding author. Telephone: (919) 513−2455. Fax: (919) 515−6302. E-mail: jfkadla@ncsu.edu.

10.1021/ma0348371 CCC: $25.00 © 2003 American Chemical Society
Published on Web 09/10/2003

**Table 1. Spinning Temperature of Lignin/PEO Blends**

| blend ratio (weight) | | spinning temp (°C) | |
|---|---|---|---|
| lignin | PEO | lignin/PEO | M-lignin/PEO |
| 100 | 0 | 208−215 | 166−170 |
| 95 | 5 | 205 | |
| 87.5 | 12.5 | 187−190 | 161−168 |
| 75 | 25 | 168−170 | 168−169 |
| 62.5 | 37.5 | 162−170 | |
| 60 | 40 | | 168−174 |
| 50 | 50 | 165 | 153−158 |
| 40 | 60 | 164−177 | 204−210 |
| 25 | 75 | 210 | 229−230 |
| 10 | 90 | 220−232 | 230−231 |
| 0 | 100 | 216−222 | 216−222 |

oxyphenol (**III**), and 2,6-dimethoxyphenol (**IV**) and phenol, were purchased from Aldrich Chemicals and recrystallized from benzene/petroleum ether (6/4).

**1-(3,4-Dimethoxyphenyl)ethanol** (**II**) was prepared by reacting 2 equiv of $NaBH_4$ (0.42 g, 11.0 mmol) with 3,4-dimethoxy acetophenone (1.0 g, 5.5 mmol) in 3:1 EtOH:$H_2O$ (50 mL) and heated under reflux for 3 h. The reaction mixture was then cooled, neutralized by bubbling $CO_2$ through the supernatant solution, and extracted with 1,2-dichloroethane (3 × 50 mL). A quantitative conversion of the acetophenone was obtained. MS *m*/*z* (relative intensity) 182 ($M^+$, 59), 167 (87), 153 (47), 139 (100), 124 (32), 108 (21), 93 (50), 77 (21), 65 (25), 51 (11), 43 (41). $^1$H NMR $\delta$ (ppm): 1.48 (d, 3H), 3.90 (d, 6H), 4.83 (q, 1H), 6.84 (q, 1H), 6.86 (q, 1H), 6.93 (d, 1H).

**3,3′-Dimethoxy-5,5′-dimethyl-[1,1′-biphenyl]-2,2′-diol** (**V**) was prepared by reacting a solution of 0.25 g (2.0 mmol) of **III** in a mixture of 5.0 mL of EtOH and 1.0 mL of 10% aqueous NaOH at 5 °C with a solution of 0.82 g (2.5 mmol) of $K_3Fe(CN)_6$ in 5 mL of water followed by 5 mL of EtOH and 1.0 mL of 10% aqueous NaOH to facilitate stirring. After 2.0 h, the reaction mixture was diluted with 50 mL of saturated $NH_4Cl$, adjusted to pH 5.5, and extracted with EtOAc, and the dried ($MgSO_4$) extract evaporated in vacuo to leave 0.21 g of crude product. Recrystallization from benzene−petroleum ether afforded colorless crystals, $T_m$ = 125 °C (DSC) $^1$H NMR $\delta$ (ppm): 2.30 (s, 6H); 3.84 (s, 6H); 6.04 (s, $D_2O$-exchangeable), 6.68 (s, 2H), 6.72 (s, 2H).

**Lignin Characterization.** Density values were determined according to the ASTM standard (D70−97) using a multivolume pycnometer 1305 (Micromeritics). Elemental analysis of the lignin samples was carried out at E & R Microanalytical Laboratories Inc. The methoxyl content was determined at our laboratory according to the modified procedure of Viebock and Schwappach.[26] Aliphatic and aromatic hydroxyl contents were determined using $^1$H NMR. Quantification was obtained from the integration ratios of aliphatic and aromatic acetoxy protons of acetylated lignin preparations relative to the internal standard, *p*-nitrobenzaldehyde.

The lignin preparations were acetylated by dissolving 200 mg of the lignin in 10 mL of pyridine−acetic anhydride (1:1, v/v) and reacted for 48 h at room temperature. The solution was poured over crushed ice and filtered. The resulting precipitate was then washed with cold water/HCl, dried, and subjected to a second acetylation treatment.

The average molecular mass and molecular mass distribution of acetylated lignin samples were determined by GPC (Waters Associates, UV and RI detectors) using styragel columns at 50 °C and THF as the eluting solvent. The GPC system was calibrated by using standard polystyrene samples. The injection volume was 100 $\mu$L, and the acetylated lignin concentration was 1 mg mL$^{-1}$ THF.

**Methylation of Lignin.** Methylation of the phenolic hydroxyl groups in lignin was performed using a diazomethane ether solution produced from *N*-methyl-*N*-nitroso-*p*-toluenesulfonamide. Accordingly, 10.0 g of lignin was suspended in dioxane/methanol (200 mL; 2:1, v/v) followed by the addition of the diazomethane ether solution (50 mL) and stirred for 3 h at room temperature. The ether phase was removed by evaporation and fresh diazomethane (20 mL) was added. Diazomethane methylation was repeated. After the final methylation, the solution was removed by evaporation and the residue was washed with diethyl ether (500 mL) and dried. The completeness of methylation was determined using the $\Delta\epsilon$ method[27] and the absence of a bathochromic shift in the UV difference spectra. In addition, $^1$H NMR analysis of acetylated methylated lignin showed no phenolic acetate groups.[28]

**Blend Preparation.** Prior to mechanical blending the lignin was thermally treated at 145 °C under vacuum for 30 min to remove volatile contaminants.[29] Blends of various PEO/lignin ratios were prepared by mechanical mixing followed by thermal extrusion using an Atlas Laboratory Mixing Extruder (Atlas Corp.). Extrusion temperatures were varied between 130 and 240 °C depending on the blend composition (Table 1).

The lignin model compound/PEO and PS blends were prepared by mixing 100 mg of polymer with 0.5 mL of a 0.2 mol L$^{-1}$ lignin model compound in $CHCl_3$ (1 mmol of lignin model compound dissolved in 5 mL of $CHCl_3$). After complete dissolution, the solvent ($CHCl_3$) was removed under reduced pressure. The blend (100 mg) was then set between glass plates and heated at 210 °C for 5 min under a $N_2$ atmosphere. The sample was then cooled to room temperature and dried in a vacuum desiccator.

**Characterization of Lignin/PEO Blends.** Mechanical properties of lignin/PEO blend fibers were estimated as tensile properties using an Instron model 4411 equipped with a 0.5 N load cell. The test speed was 0.5 mm min$^{-1}$, and the sample length was 25 mm. Tensile tests were performed at constant temperature (25 °C) and relative humidity (65%). All reported results are the average of 20 tests.

Glass transition temperatures, $T_g$, of the blends were determined on a TA Instruments Q 100 DSC with a scan rate of 20 °C/min over the temperature range of −90 to 200 °C. The measurements were made using 4−5 mg samples under a nitrogen atmosphere after the samples were quickly cooled to −90 °C. The glass transition temperature was recorded as the midpoint temperature of the heat capacity transition of the second heating run. Samples were run in duplicate and are reported as the average of the two runs and were within experimental error of each other (±1.0 °C).

The equilibrium melting point, $T_m^{eq}$, was determined by DSC using Hoffman−Weeks plots.[30] In a typical experiment, 5.0 mg samples, as weight fractions of PEO, were heated to 90 °C and maintained at this temperature for 10 min to completely eliminate PEO crystallinity. The sample was than quenched to the desired isothermal crystallization temperature, $T_{ic}$, and held at temperature for 2 h to allow complete crystallization. After isothermal crystallization, the melting temperature, $T_m'$, was measured using a heating rate of 10 °C min$^{-1}$; $T_m'$ was determined as the peak top temperature.

Infrared (FT-IR) spectra of the polymer blends were determined using the diffuse reflectance (DRFT-IR) method (due to the physical properties of the polymer blends it was difficult to prepare uniform KBr pellets for FT-IR analysis using transmittance detection). The polymer blends (10 mg) were dispersed in KBr (200 mg), and DRFT-IR measurements were recorded on a Perkin-Elmer 16PG FT-IR spectrometer; 256 scans were collected with a spectral resolution of 2.0 cm$^{-1}$. Owing to the hygroscopic nature of the polymer blends, a pure nitrogen flow was maintained over the sample during collection. FT-IR analysis of the model compounds was performed in $CCl_4$ using a liquid cell with ZnSe windows and a 1 mm path length, 16−32 scans were acquired at a spectral resolution of between 2.0 and 4.0 cm$^{-1}$.

## Results and Discussion

**Preparation of Lignin/PEO Blend Fibers.** Extrusion temperatures of the lignin/PEO blends are listed in Table 1. All samples exhibited good thermal processing properties. Extrusion temperature was dependent on blend composition, with the lowest temperature observed in the middle range of the blending ratio.

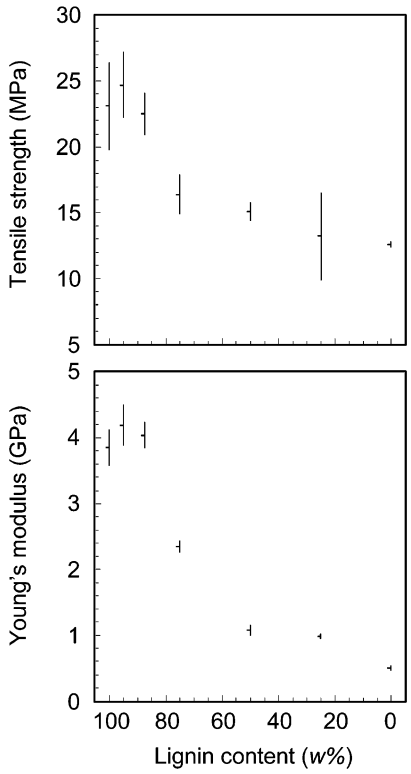


**Figure 1.** Tensile strength and Young's modulus of lignin/PEO blend fibers.

**Table 2. Physical Properties of Lignin/PEO Blend Fibers**

| blend ratio (weight) | | diameter | tensile strength | Young's modulus | elongation |
|---|---|---|---|---|---|
| lignin | PEO | ($\mu$m) | (MPa) | (GPa) | (%) |
| 100 | 0 | 148 ± 25 | 23.1 ± 3.3 | 3.85 ± 0.27 | 0.6 ± 0.1 |
| 95 | 5 | 162 ± 11 | 24.7 ± 2.5 | 4.19 ± 0.31 | 0.6 ± 0.1 |
| 87.5 | 12.5 | 163 ± 21 | 22.5 ± 1.6 | 4.04 ± 0.20 | 0.6 ± 0.1 |
| 75 | 25 | 151 ± 7 | 16.4 ± 1.5 | 2.35 ± 0.08 | 0.8 ± 0.1 |
| 50 | 50 | 185 ± 27 | 15.1 ± 0.7 | 1.07 ± 0.08 | 3.5 ± 0.5 |
| 25 | 75 | 114 ± 5 | 13.2 ± 3.3 | 0.98 ± 0.04 | 19.7 ± 3.7 |
| 0 | 100 | 274 ± 16 | 12.6 ± 0.2 | 0.51 ± 0.03 | 5.4 ± 0.6 |

The Young's modulus (3.9 GPa), tensile strength (23 MPa) and elongation (0.6%) of the lignin-based blends increased slightly with addition of low wt % additions of PEO (Table 2). Incorporation of 5 wt % of PEO increased the corresponding values to 4.2 GPa, 25 MPa, and 0.6%, respectively (Figure 1). Increasing addition of PEO reduced both the Young's modulus and tensile strength of the lignin-based thermoplastics, decreasing dramatically at PEO levels of 25−50 wt %. The initial increase in tensile behavior is likely the result of PEO disrupting the intermolecular association of the lignin macromolecules; the physical properties of lignin-based materials are determined by the extent of lignin intermolecular association and formation of supramacromolecular complexes.[31] Through specific intermolecular interactions between PEO and individual lignin components, the supramacromolecular lignin complexes dismantle. Increasing PEO incorporation further disrupts the supramacromolecular lignin structure and the observed physical properties become more strongly influenced by the PEO component. At 75 wt % PEO, the lignin/PEO blend exhibits a substantial increase in elongation, 19.7%, compared with 0.6% and 5.4% for lignin and PEO, respectively. This large change in ductility suggests the elimination of the supramacromolecular lignin complexes and the formation of specific

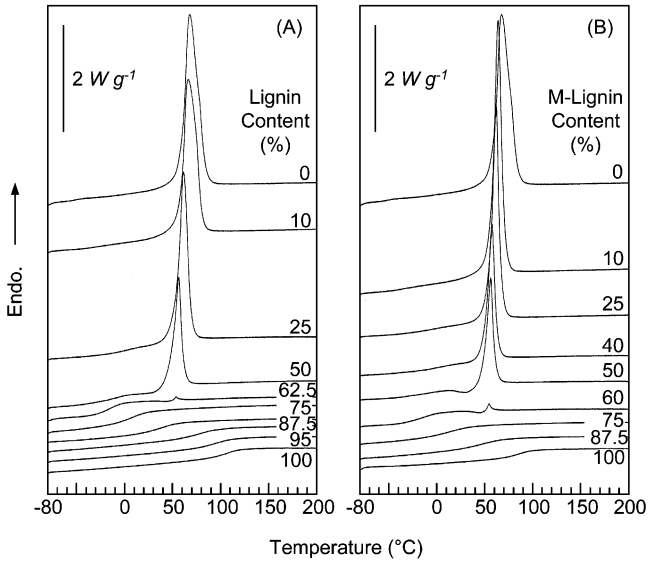


**Figure 2.** DSC curves of lignin/PEO (A) and M-lignin/PEO (B) blend fibers.

**Table 3. Chemical Properties of Hardwood Kraft Lignin**

| functional goups (mmol g$^{-1}$) | | | | | |
|---|---|---|---|---|---|
| hydroxyl | | | | molecular mass | |
| aliphatic | phenolic | methoxyl | S G$^{-1}$ | $M_w$ | dispersity |
| 4.1 | 4.3 | 5.8 | 1.2 | 2400 | 1.8 |

interactions between components: consistent with a miscible polymer blend system.[32]

**Analysis of Intermolecular Interactions between PEO and Lignin.** Lignin, a polyol, has both phenolic and aliphatic hydroxyl groups (Table 3) that can participate in hydrogen-bonding with PEO (vide infra). To investigate the role of the various hydroxyl groups and to characterize the hydrogen-bonding interactions between lignin and PEO, the phenolic hydroxyl groups in lignin were selectively methylated using diazomethane.[33] The methylated lignin (M-lignin) was then blended with PEO under the same conditions as those used in the unmethylated lignin blends.

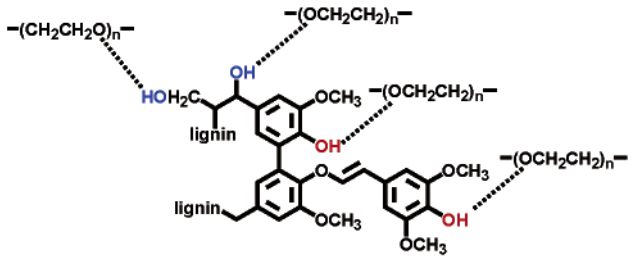


**Thermal Analysis.** Differential scanning calorimetry (DSC) is extensively used to investigate miscibility in polymer blends. A single compositional-dependent glass transition temperature ($T_g$) is an indication of full miscibility at a dimensional scale between 5 and 15 nm.[11] Figure 2 shows DSC analyses of the lignin/PEO and M-lignin/PEO blends of various compositions. The pure amorphous lignins exhibit one $T_g$ at 106 and 86 °C, respectively. In both systems, the $T_g$ decreases in temperature with increasing PEO blend content. Similarly, the melting temperature ($T_m$) of the PEO component in the blends decreases with the increase of lignin content. Table 4 summarizes the thermal properties of PEO, lignin, M-lignin, and the corresponding polymer blends.

**Table 4. DSC Results of the Lignin/PEO and M-Lignin/PEO Blend Fibers**

| blend ratio (weight) | | lignin/PEO blend | | | | | M-lignin/PEO blend | | | | |
|---|---|---|---|---|---|---|---|---|---|---|---|
| lignin | PEO | $T_g$ (°C) | $\Delta C_p$ (J g$^{-1}$ C$^{-1}$) | $T_m$ (°C) | $\Delta H$ (J g$^{-1}$) | crystallinity (%) | $T_g$ (°C) | $\Delta C_p$ (J g$^{-1}$ C$^{-1}$) | $T_m$ (°C) | $\Delta H$ (J g$^{-1}$) | crystallinity (%) |
| 1 | 0 | 106 | 0.60 | × | 0 | 0 | 86 | 0.53 | × | 0 | 0 |
| 0.95 | 0.05 | 95 | 0.61 | × | 0 | 0 | *a* | *a* | *a* | *a* | *a* |
| 0.875 | 0.125 | 76 | 0.68 | × | 0 | 0 | 48 | 0.71 | × | 0 | 0 |
| 0.75 | 0.25 | 38 | 0.77 | × | 0 | 0 | 13 | 0.75 | × | 0 | 0 |
| 0.625 | 0.375 | 5 | 0.85 | × | 0 | 0 | *a* | *a* | *a* | *a* | *a* |
| 0.6 | 0.4 | *a* | *a* | *a* | *a* | *a* | −15 | 0.62 | 54 | 2 | 3 |
| 0.5 | 0.5 | −15 | 0.73 | 53 | 1 | 1 | −7 | 0.35 | 56[b] | 56[b] | 60[b] |
| 0.4 | 0.6 | −7[b] | 0.49[b] | 56 | 63 | 56 | 4[b] | 0.24[b] | 57 | 73 | 65 |
| 0.25 | 0.75 | 4[b] | 0.26[b] | 61 | 112 | 80 | −5[b] | 0.25[b] | 61 | 113 | 80 |
| 0.1 | 0.9 | −2.4 | 0.18 | 66 | 146 | 86 | −35 | 0.12 | 63 | 145 | 86 |
| 0 | 1 | −50 | 0.11 | 67 | 168 | 90 | −50 | 0.11 | 67 | 168 | 90 |

[a] No sample. [b] There are some difficulties in assigning the thermal transition point because the melting or recrystallization peak is partially overlapped with the glass-transition state and the melting peak.

The detection of a single $T_g$ via thermal analysis provides important information as to the composition of the individual amorphous phases present in the material. All lignin/PEO and M-lignin/PEO blends show only a single $T_g$ over the entire blend composition. The single $T_g$ strongly suggests that these are fully miscible blends with a homogeneous amorphous phase. In general, the formation of miscible binary polymer blends depends on the occurrence of exothermic interactions between the two components being mixed.[10] The manner in which the glass transition temperature varies with blend composition is reflective of the relative strengths of these intermolecular interactions. Several theoretical and empirical equations have been proposed for the prediction of $T_g$ in miscible polymer blends, based on the composition of the blend, the $T_g$s of the individual components, and the nature of the interactions between these components.[16,20,21,23] Of these, Lu and Weiss[21] derived a general expression for the $T_g$ of a binary polymer mixture ($T_{gm}$) wherein the other popularly used equations were shown to be special cases within their theory. The equation included no adjustable parameters and utilized entropy as the thermodynamic variable. The enthalpy of mixing for the blend ($\Delta H_m$) was related to the Flory−Huggins interaction parameter ($\chi$) through the van Laar relationship $\Delta H_m = \chi RT\phi_1\phi_2$, where $\phi_I$ is the volume fraction of component $i$, $R$ is the gas constant and $T$ the temperature. The Flory−Huggins interaction parameter ($\chi$) was assumed to be a quadratic function of composition; $\chi = \chi_o + \chi_1 w_2 + \chi_2 w_2^2$ where $w_2$ is the weight fraction of polymer 2. Similarly, the isobaric specific heat of the mixture ($c_{pm}$) was assumed to have the form $c_{pm} = x_1 c_{p1} + x_2 c_{p2} + x_1 x_2 \delta c_p$, where $x_i$ is the mole-fraction of polymer $i$, $c_{pi}$ the isobaric specific heat of component $i$, and $\delta c_p$ is the change in specific heat due to mixing (which is negative for a miscible blend).[34] The resulting equations are[21]

$$T_{gm} = \frac{(w_1 T_{g1} + k w_2 T_{g2})}{(w_1 + k w_2)} + \frac{A w_1 w_2}{(w_1 + k w_2)(w_1 + b w_2)(w_1 + c w_2)^2}$$

$$A = \frac{-\chi R (T_{g1} - T_{g2}) c}{M_1 \Delta c_{p1}} \qquad k = \frac{\Delta c_{p2} - w_1 \delta c_p^l}{\Delta c_{p1} - w_2 \delta c_p^g}$$

where $b = M_2/M_1$, ($M_i$ is the molar mass per chain segment of polymer $i$), $c = \rho_1/\rho_2$ ($\rho_i$ is the density of polymer $i$), $w_i$ is the weight fractions of polymer $i$, and $\Delta c_{pi} = c_{pi}^l - c_{pi}^g$ at $T_{gi}$ (the change in specific heat of polymer $i$), superscripts g and l denoting the glassy and liquid states, respectively.

In polymer blends characterized by weak intermolecular interactions between the miscible polymer blend components, the effect of $k$ is greater than $A$,[21] and the equation is simplified to the Gordon−Taylor equation:[20]

$$T_{gm} = \frac{(w_1 T_{g1} + k' w_2 T_{g2})}{(w_1 + k' w_2)}$$

Here

$$k' = k + A/(T_{g2} - 1)$$

and $k'$ can be employed qualitatively as a measure of the intermolecular interactions in the polymer blend.[21] By contrast, in polymer blends with strong intermolecular interactions, the magnitudes of $k$, $b$, and $c$ are such that $T_{gm}$ may be quantified by Kwei's equation:[22]

$$T_{gm} = \frac{(w_1 T_{g1} + k w_2 T_{g2})}{(w_1 + k w_2)} + A' w_1 w_2$$

where

$$k = \frac{\Delta c_{p2}}{\Delta c_{p1}}$$

In this case, $A'$ may be regarded as measure of the interactions between polymer components.

The Lu and Weiss equation satisfactorily predicts $T_g$−composition curves for miscible polymer blends that exhibit either positive or negative deviations from a linear mixing rule, depending on the strength of interaction.[21] Figure 3 shows the $T_g$-composition curves for the lignin/PEO and M-lignin/PEO blends. Both polymer blend systems exhibit negative deviation from linear mixing and is satisfactorily predicted by the Lu and Weiss equation (solid line in Figure 3) as well as the Kwei equation (dotted line in Figure 3). The Gordon−Taylor equation did not produce a satisfactory fit of the experimental data (dashed line in Figure 3). Table 5 lists the fitting parameters obtained from the various theoretical and empirical equations used to predict $T_g$ of miscible polymer blends.

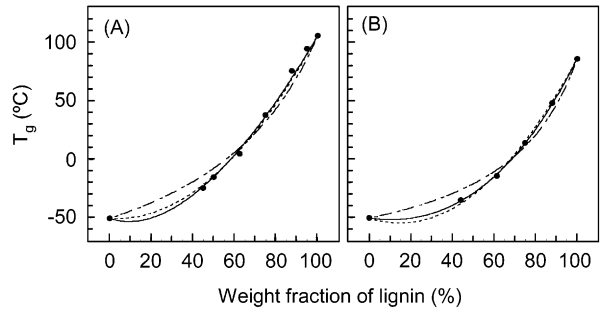


**Figure 3.** $T_g$ of lignin/PEO (A) and M-lignin/PEO (B) blend fibers: solid line, Lu and Weiss; dotted line, Kwei; dashed line, Gordon−Taylor.

The calculated values of $\chi$ from the Lu and Weiss equation (−0.34 and −0.15 for the lignin and M-lignin PEO blends, respectively) indicate relatively strong intermolecular interactions, wherein the lignin, containing the phenolic hydroxyl groups, forms stronger intermolecular interactions with PEO than the M-lignin, with only aliphatic hydroxyl groups available.

The observed $T_g$ phenomenon, which is related to segmental motions in the polymer, is affected by steric hindrance and variations of the flexibility of the polymer chains.[23,35] As a result, $A'$ has been related to both hydrogen bond formation and to changes in the environment of the polymer chains. The methylation of the phenolic hydroxyl groups within the lignin macromolecule decreases the extent of intra and intermolecular interactions within lignin, increasing the molecular mobility or flexibility of the polymer chains and results in the observed lower $T_g$ of the M-lignin relative to the original lignin. Therefore, the lower value of $A'$ ($A' = -170$ for the lignin/PEO cf. $A' = -193$ for M-lignin/PEO blends) for the M-lignin/PEO blend indicates a lower propensity to hydrogen-bonding than that of the lignin/PEO blends.[36]

**Equilibrium Melting Temperature and Melting Point Depression.** The depression of the melting point of a crystalline polymer blended with an amorphous polymer provides important information about its miscibility and its associated polymer−polymer interaction parameter ($\chi$). The temperature reduction is caused by thermodynamic depression arising from a reduction in chemical potential due to the presence of the polymeric *solvent*. When two polymers are miscible in the molten state, the chemical potential of the crystallizable polymer is decreased due to the addition of the second component. This leads to a reduction in the equilibrium melting temperature with increasing amorphous polymer content, especially in blends containing specific interactions between components. An immiscible blend will typically not show the depression of the equilibrium melting point. Using the equation of Nishi and Wang,[37] which is based on the Flory−Huggins theory,[10] the melting point depression is given by the following equation:[10,37]

$$\Delta T_m = T_m^0 - T_{m2}^0 = -T_m^0\left(\frac{V_{2u}}{\Delta H_{2u}}\right)B\phi_1^2$$

Subscripts 1 and 2 represent the amorphous and the crystalline polymers, respectively, $T_m^0$ is the equilibrium melting point of the pure crystallizable component, $T_{m2}^0$ is the equilibrium melting point of the blend, $\phi$ is the volume fraction, $V_u$ is the molar volume of the repeating units, $\Delta H_u$ is the heat of fusion per mole of repeat unit, and $B$ refers to the interaction energy density characteristic of the polymer pair, and is, in practice, related to the thermodynamic interaction parameter $\chi_{12}$ by $B = RT_m^0(\chi_{12}/V_{1u})$.

To determine the equilibrium melting temperatures for PEO ($T_m^0$) and the polymer blends ($T_{m2}^0$) of given compositions, and to eliminate the morphological effect from the melting point depression, the method of Hoffman and Weeks was used.[30] However, as discussed and demonstrated by many groups,[38,39] the errors associated with the Hoffman−Weeks approach could be

**Table 5. Equations for $T_g$ Variations with Blend Composition of Lignin/PEO Blend Fibers**

| author(s) | equation | parameter: lignin/PEO | parameter: M-lignin/PEO |
|---|---|---|---|
| Fox | $\frac{1}{T_g} = \frac{w_1}{T_{g1}} + \frac{w_2}{T_{g2}}$ | − ($R^2 = 0.927$) | − ($R^2 = 0.807$) |
| Couchman | $\ln T_g = \frac{w_1\Delta c_{p1}\ln T_{g1} + w_2\Delta c_{p2}\ln T_{g2}}{w_1\Delta c_{p1} + w_2\Delta c_{p2}}$ | − ($R^2 = 0.936$) | − ($R^2 = 0.894$) |
| Gordon-Taylor | $T_g = \frac{w_1 T_{g1} + k w_2 T_{g2}}{w_1 + k w_2}$ | $k = 0.37 \pm 0.04$ ($R^2 = 0.982$) | $k = 0.27 \pm 0.03$ ($R^2 = 0.988$) |
| Kwei | $T_g = \frac{w_1 T_{g1} + k w_2 T_{g2}}{w_1 + k w_2} + A w_1 w_1$ | $q = -170 \pm 8$, $k = 1$ ($R^2 = 0.996$) | $q = -193 \pm 4$, $k = 1$ ($R^2 = 0.999$) |
| Lu−Weiss | $T_g = \frac{w_1 T_{g1} + k w_2 T_{g2}}{w_1 + k w_2} + \frac{A w_1 w_2}{(w_1 + k w_2)(w_1 + b w_2)(w_1 + c w_2)^2}$ <br> $A = -\frac{\chi R(T_{g1} - T_{g2})c}{M_1\Delta c_{p1}}$ k $= \frac{\Delta c_{p2} - w_1\delta c_p^l}{\Delta c_{p1} - w_2\delta c_p^g}$ | $\chi = -0.34$, $k = 1.9$ ($R^2 = 0.997$) | $\chi = -0.15$, $k = 0.8$ ($R^2 = 0.999$) |

[a] Here $T_g$, $T_{g1}$, and $T_{g2}$ are glass transition temperature of the blend and homopolymers, respectively. $w_1$ and $w_2$ are the corresponding weight fractions. $\Delta c_{p1}$ and $\Delta c_{p2}$ are the magnitudes of increase in heat capacity at $T_g$ of the corresponding homopolymers. $b$ and $c$ in the Lu and Weiss equation are ratios of density, $\rho_1/\rho_2$, and molar mass of repeating unit, $M_2/M_1$, of homopolymers.

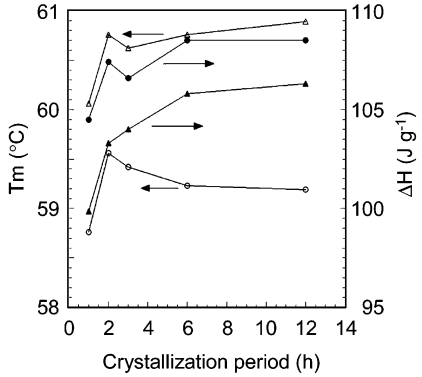


**Figure 4.** $T_m$ and $\Delta H$ values of lignin/PEO = 25/75 blend as a function of the crystallization time. Triangle and circle symbols are samples crystallized at 45 and 35 °C, respectively.

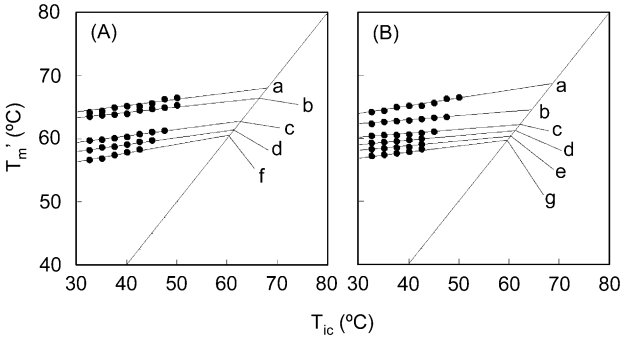


**Figure 5.** Hoffman−Weeks plot for isothermally crystallized lignin/PEO (A) and M-lignin/PEO (B) blend fibers: (a) 0/100; (b) 10/90; (c) 25/75; (d) 32.5/67.5; (e) 35/65; (f) 40/60; (g) 50−50.

significant, and a small uncertainty in melting point could profoundly affect the value of $\chi$. In certain blends, the appearance of a melting point depression may in fact be the result of incomplete crystallization, rather than thermodynamic considerations. This is particularly the case in polymer blend systems with very small melting point depressions. The effect of crystallization time on the observed melting point was determined for our blend systems and is illustrated in Figure 4. The $T_m$ of the PEO fraction in lignin/PEO = 25/75 blend is independent from crystallization period, if that period is longer than 2 h. This behavior is observed for both high and low crystallization temperatures, 45 and 35 °C, respectively. The difference in observed $T_m$ between crystallization times of 2 and 12 h was measured to be less than 0.5 °C (within experimental error of the instrument used—DSC analysis). The observed $\Delta H$ value at 2 h is >95% of relative $\Delta H$ value for a crystallization time of 12 h. Therefore, all $T_m$ measurements were made using crystallization times of 2 h and with relative $\Delta H$ values within 95% of the maximum $\Delta H$ obtained for that blend.

Figure 5 presents the Hoffman−Weeks plot to obtain the equilibrium melting points for pure PEO, the lignin/PEO (A) and the M-lignin/PEO (B) blends. The experimental results were fit using $T'_m = \sigma T_{ic} + (1 - \sigma) T^0_m$,[30,37] where $\sigma$ is a stability parameter[37] which is usually related to morphological factors, and $T_{ic}$ is the isothermal crystallization temperature. The values of $T^0_m$ for PEO and its blends with the lignin were obtained by the extrapolation procedure using a least-squares fit of the data to the intersection with $T'_m = T_{ic}$. Assuming $B$ or $\chi$ is composition independent, a plot

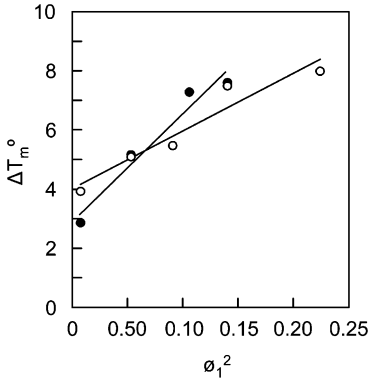


**Figure 6.** Equilibrium melting point depression of PEO in blends: (●) lignin blend; (○) M-lignin blend.

of the melting point depression, $\Delta T_m$, vs the square of the volume fraction of lignin, $\phi_1^2$ (Figure 6), produces a $B$ value of −5.5 cal cm$^{-3}$ for the lignin/PEO blend and −2.9 cal cm$^{-3}$ for the M-lignin/PEO blend ($\Delta H_{2u}$ = 1.980 kcal/mol and $V_{2u}$ = 38.1 cm$^3$/mol [40]). The negative $B$ value is consistent with a miscible system, and is comparable to results obtained from Phenoxy/PEO blends ($B$ = −6.2 cal cm$^{-3}$).[41] However, the $T^0_m$ depression plots for both the lignin/PEO and M-lignin/PEO blends deviate from a linear line. This may suggest a composition dependence of $\chi$, and therefore, $\chi$ values could not be calculated, for these systems. Nonetheless, a melting point depression is clearly observed (Table 4) for both polymer blend systems, suggesting a negative value for $\chi$[40] and a stronger interaction between the lignin/PEO blends than the M-lignin/PEO blends.

**Fourier Transform Infrared Spectroscopy Analysis.** Infrared spectroscopy has been proven to be a highly effective means of investigating specific interactions between polymers. FT-IR can be used to qualitatively and quantitatively study the mechanism of interpolymer miscibility through hydrogen-bonding. To further understand the thermodynamic behavior of the lignin-based/PEO blends the intermolecular interactions of PEO with lignin and M-lignin was investigated with FT-IR.

Figure 7 shows the FT-IR spectra of the hydroxyl-stretching ($\nu_{O-H}$) region (3100−3700 cm$^{-1}$) of lignin (A) and M-lignin (B) and the respective PEO blends. Owing to the variety of intra- and intermolecular hydrogen bonds within and between lignin macromolecules a broad $\nu_{O-H}$ band is observed for both lignins. The lignin spectrum has a broad band center at ∼3422 cm$^{-1}$ with an apparent shoulder at ∼3518 cm$^{-1}$. These bands are assigned to the average stretching of intermolecular hydrogen bonding and intramolecular hydrogen bonding, respectively. The M-lignin exhibits the same broad band center at ∼3422 cm$^{-1}$, but the shoulder at ∼3518 cm$^{-1}$ is less pronounced.

Blending with PEO dramatically changes the $\nu_{O-H}$ region of the lignin. In the lignin/PEO blends (Figure 7A) the broad center band shifts to lower wavenumber with increasing PEO content, and a third band center appears at ∼3295 cm$^{-1}$. The relative intensity of this band increases with increasing PEO content, and the shape of the $\nu_{O-H}$ region becomes broader. In contrast, the broad center band in the M-lignin/PEO blends does not shift, and less change in the overall $\nu_{O-H}$ region is observed (Figure 7B).

A corresponding effect is observed in the asymmetric C−O−C stretching ($\nu_{as(C-O-C)}$) region (1050−1150 cm$^{-1}$)

**Table 6. IR Bands ($cm^{-1}$) of Free, Intramolecular, and Intermolecular Hydroxyl Groups of Lignin Model Compounds**

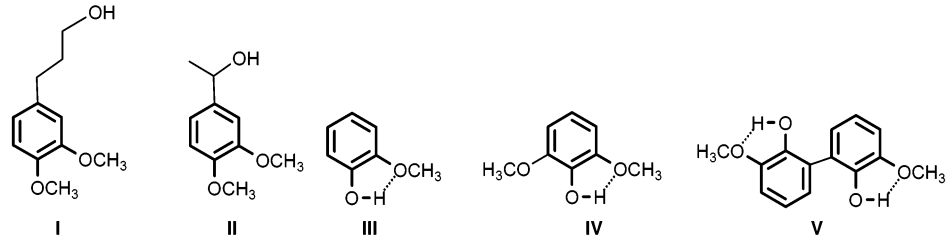


| | lignin model compounds | | | | | |
|---|---|---|---|---|---|---|
| | **I** | **II** | **III** | **IV** | **V** | phenol |
| free hydroxyl group[a] | 3639 (s)[c] | 3616 (s) | | | | 3611(s) |
| intramolecular hydrogen bond | | | 3556 (s) | 3554 (s) | 3552 (s) | |
| intermolecular hydrogen bond[b] (dimer) | 3500 (B) | 3484 (B) | 3508 (s) | 3490 (s) | nondetect | nondetect |
| intermolecular hydrogen bond[b] (multimer) | 3390 (B) | 3416 (B) | 3444 (s) | 3458 (s) | 3219 (B) | 3226 (B) |

[a] IR band for free and intramolecular hydrogen bond was measured in diluted $CCl_4$ solution (0.01 mol $L^{-1}$). [b] Intermolecular hydrogen bonds were estimated from band center of nondiluted sample. The model compound was melt spread on a ZnSe plate at 150 °C for 5 min under nitrogen atmosphere. [c] Key: (s) strong; (B) broad.

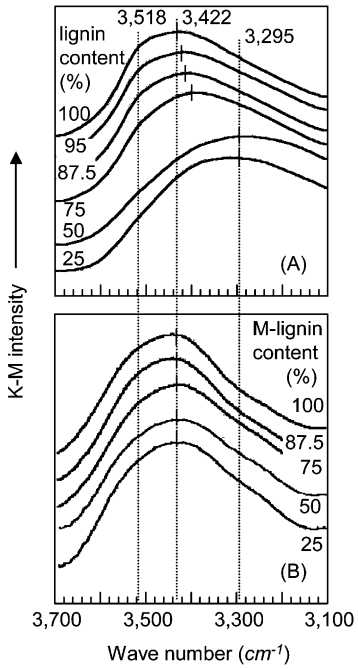


**Figure 7.** DR−FTIR spectra of lignin/PEO (A) and M-lignin/PEO (B) blends in the $\nu_{OH}$ region.

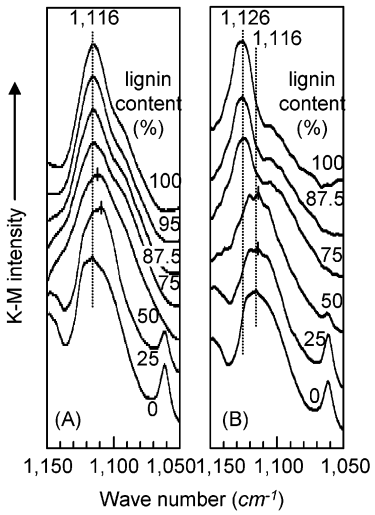


**Figure 8.** DR−FTIR spectra of lignin/PEO (A) and M-lignin/PEO (B) blend fibers in the $\nu_{(C-O-C)\ asym}$ region.

of the blends. As shown in Figure 8A, the $\nu_{as(C-O-C)}$ band of lignin and PEO appear at the same position (1116 $cm^{-1}$). However, the observed $\nu_{as(C-O-C)}$ band center appears at a lower wavenumber in the lignin/PEO 50/50 (1111 $cm^{-1}$) and 25/75 (1109 $cm^{-1}$) blends, consistent with the observed effect in the $\nu_{O-H}$ region. The $\nu_{as(C-O-C)}$ band of the M-lignin/PEO blends is shown in Figure 8B. Unlike the original lignin, the $\nu_{as(C-O-C)}$ band of the M-lignin appears at a higher wavenumber, 1126 $cm^{-1}$ relative to that of PEO. Moreover, there appears to be no significant shift in the band center associated with this region with increasing blend ratio. Therefore, the large change in the $\nu_{O-H}$ region of the lignin/PEO blends relative to the M-lignin/PEO blends, along with the differences between the $\nu_{as(C-O-C)}$ regions, suggests the formation of strong hydrogen bonds between the phenolic hydroxyl groups and PEO.

The band envelopes of the lignin, M-lignin and corresponding blends (Figure 7) are a complex superposition of various types of OH- - -O hydrogen bonds. To resolve and further interpret the observed differences in hydrogen bonding between the two systems (lignin/PEO vs M-lignin/PEO), FT-IR studies were performed using various lignin model compounds. Table 6 lists the $\nu_{O-H}$ bands for various lignin model compounds with differing phenolic and aliphatic hydroxyl groups. Infrared bands for "free" or non-hydrogen-bonded hydroxyl stretching modes were only observed in dilute solutions of the aliphatic hydroxyl group containing model compounds **I** and **II**; the phenolic compounds (**III**−**V**) form a strong intramolecular hydrogen-bond with the adjacent methoxyl group even under dilute solution conditions. At high concentration (Figure 9A), and in the solid state, all of the lignin model compounds formed various intermolecular hydrogen-bonding complexes (dimer ∼3500 $cm^{-1}$ and multimer ∼3400 $cm^{-1}$).

Blending the various lignin model compounds with PEO revealed distinct differences in hydrogen-bonding patterns (Figure 9B). Compounds **I** and **II** exhibited similar band envelopes centered at ∼3450−3490 $cm^{-1}$. These spectra showed slight differences to that observed for the lignin model compounds in the absence of PEO (Figure 9A); the band envelope sharpened, indicating a less complex hydrogen-bonding system. The absence of a shift in wavenumber indicates the strength of the hydrogen bond between aliphatic hydroxyl groups such

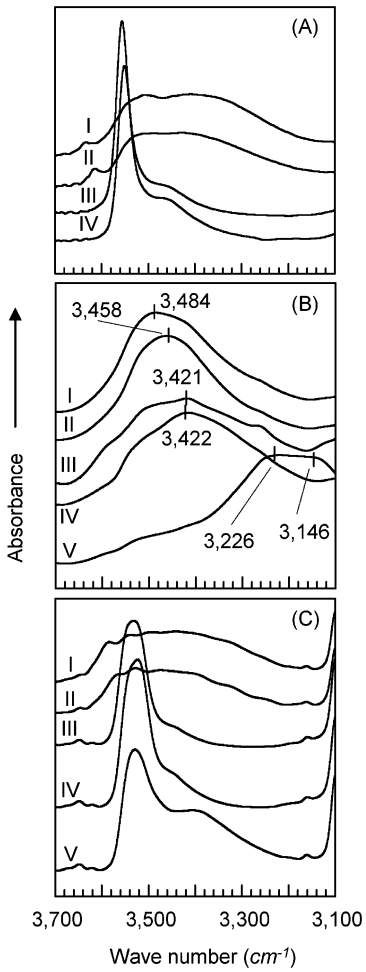


**Figure 9.** FTIR spectra of lignin model compounds collected in $CCl_4$ (A), PEO (B), and PS (C) in the $\nu_{OH}$ region.

as those found in lignin (**I** and **II**) and PEO are of the same magnitude as those between such groups within lignin itself. These results are consistent with, and support the findings wherein the band envelope of the $\nu_{O-H}$ region for the M-lignin/PEO blends (Figure 7B) did not substantially change with the incorporation of PEO.

The monoaromatic phenolic compounds **III** and **IV** had similar band envelopes centered at ~3420 $cm^{-1}$ (Figure 9B). However, unlike compounds **I** and **II**, the band envelopes of **III** and **IV** are much broader and centered at a lower wavenumber in the presence of PEO. This result suggests a change in hydrogen-bonding in which a stronger, more complex hydrogen-bonding system is formed. Interestingly, the addition of PEO to compound **V** showed not only a shift in wavenumber, but also a sharpening of the band envelope; two discernible band centers at 3226 and 3146 $cm^{-1}$, respectively, are present.

FT-IR analysis of the lignin model compounds shows the presence of strong hydrogen bonds between the various hydroxyl groups present (Figure 9A). PEO (Figure 9B) appears to interact with the phenolic hydroxyl moieties (compounds **III**−**V**) to a greater and different extent than that of the aliphatic hydroxyl moieties (compounds **I** and **II**), consistent with the lignin/PEO and M-lignin/PEO blends. To confirm the observed change in the hydroxyl stretching bands upon polymer addition is due to specific interactions between lignin and PEO and not the result of enhanced intermolecular interactions between lignin macromolecules as a result of dilution with the synthetic polymer FT-IR analysis of lignin model compound/polystyrene (PS) blends (Figure 9C) were performed. Unlike the PEO blends (Figure 9B), incorporation of PS produces a very broad band envelope for compounds **I** and **II**, whereas for **III**, **IV**, and **V** very sharp $\nu_{O-H}$ bands are observed. In fact, the FT-IR spectra of the various lignin model compound blends with PS (Figure 9C) are identical to FT-IR spectra obtained from similar concentration lignin model compound solutions in carbon tetrachloride (Figure 9A).

Purcell and Drago[25] have shown that the wavenumber shift ($\Delta\nu_{O-H}$) between the free hydroxyl stretching vibration and that of hydrogen-bonded species yields a measure of the average strength of the intermolecular interactions. From the lignin model compounds investigated it can be seen that very strong intermolecular interactions exist between the various hydroxyl groups in lignin (Table 6) as well as in lignin/PEO blends. In fact, in the pure lignin and the M-lignin/PEO blends $\Delta\nu_{O-H} \approx 189$ $cm^{-1}$, whereas in the lignin/PEO blends $\Delta\nu_{O-H}$ increases to about 316 $cm^{-1}$ (a corresponding wavenumber shift in the C−O−C stretching region in PEO is also observed, $\Delta\nu_{C-O-C} \approx 10$ $cm^{-1}$). This suggests that the average hydrogen bond between the ether oxygen in PEO and the phenolic hydroxyl groups in lignin is stronger than with the aliphatic hydroxyl groups and that the hydrogen-bonds involving aliphatic hydroxyl groups are similar to those within the lignin homopolymer itself.

## Summary

Lignin-based thermoplastic blends have been produced using a commercial technical lignin and PEO. Incorporation of small amounts of PEO (5−10% w/w) sufficiently disrupts the lignin supramacromolecular complexes leading to enhanced physical properties. Increasing PEO incorporation further disrupts the supramacromolecular lignin structure and the observed physical properties become more influenced by the PEO component. Miscible blends were observed over the entire blend ratio. The basis for the miscibility is hydrogen-bonding interactions between the hydroxyl protons of lignin and the proton accepting sites of PEO. The strength of the hydrogen-bonding interactions observed is different for the aromatic and aliphatic hydroxyl groups in lignin. FT-IR analyses revealed a strong hydrogen bond between the aromatic hydroxyl proton and the ether oxygen in PEO; no such hydrogen bond was observed in the lignin involving only aliphatic hydroxyl group hydrogen-bonding. However, a negative deviation of $T_g$ from the weight-average values was observed in both blend systems, suggesting a polymer blend system involving weak specific intermolecular interactions. This apparent contradiction may be explained by the following: (i) the number or extent of hydrogen-bonding present may be relatively low, as suggested by the Kwei fitting parameters, and/or (ii) although strong intermolecular hydrogen-bonding exists, the effect of PEO incorporation on blend $T_g$ may depend on the nonbonding interactions that are responsible for the supramacromolecular complexes present in lignin-based systems.

**Acknowledgment.** Financial support from North Carolina State University and the US Department of Agriculture is gratefully acknowledged.

## References and Notes


(1) Imam, S. H.; Greene, R. V.; Zaidi, B. R. *Biopolymers: utilizing nature's advanced materials*; American Chemical Society: Washington, DC, 1999.
(2) Martuscelli, E.; Palumbo, R.; Kryszewski, M.; Galeski, A. *Polymer blends: processing, morphology, and properties: proceedings of the First Joint Italian-Polish Seminar on Multicomponent Polymeric Systems, held in Capri, Italy, October 16−21, 1979*; Plenum Press: New York, 1980.
(3) Feldman, D.; Banu, D.; Lacasse, M.; Wang, J.; Luchian, C. *J. Macromol. Sci.—Pure Appl. Chem.* **1995**, *A32*, 1613−1619.
(4) Tudorachi, N.; Cascaval, C. N.; Rusu, M. *J. Polym. Eng.* **2000**, *20*, 287−304.
(5) Yamane, H. *Nihon Reoroji Gakkaishi* **1999**, *27*, 213−218.
(6) Glasser, W. G.; Sarkanen, S. *Lignin: properties and materials*, American Chemical Society: Washington, DC, 1989.
(7) Meister, J. J.; Chen, M.-j. U.S. Patent 5,424,382, 1995.
(8) Li, Y.; Mlynar, J.; Sarkanen, S. *J. Polym. Sci., Part. B: Polym. Phys.* **1997**, *35*, 1899−1910.
(9) Wang, J. S.; Manley, R. S.; Feldman, D. *Prog. Polym. Sci.* **1992**, *17*, 611−646.
(10) Flory, P. J. *Principles of polymer chemistry*; Cornell University Press: Ithaca, NY, 1953.
(11) Paul, D. R.; Bucknall, C. B. *Polymer blends*; Wiley: New York, 2000.
(12) Wang, J.; Cheung, M. K.; Mi, Y. L. *Polymer* **2002**, *43*, 1357−1364.
(13) Oulevey, F.; Burnham, N. A.; Gremaud, G.; Kulik, A. J.; Pollock, H. M.; Hammiche, A.; Reading, M.; Song, M.; Hourston, D. J. *Polymer* **2000**, *41*, 3087−3092.
(14) Ilzhoefer, J. R.; Spontak, R. J. *Langmuir* **1995**, *11*, 3288−3291.
(15) Schantz, S. *Macromolecules* **1997**, *30*, 1419−1425.
(16) Couchman, P. R. *Macromolecules* **1978**, *11*, 1156−1161.
(17) Couchman, P. R. *Macromolecules* **1987**, *20*, 1712−1717.
(18) Couchman, P. R. *Macromolecules* **1991**, *24*, 5772−5774.
(19) Dimarzio, E. A.; Gibbs, J. H. *J. Polym. Sci.* **1959**, *40*, 121−131.
(20) Gordon, M.; Taylor, J. S. *J. Appl. Chem.* **1952**, *2*, 493−500.
(21) Lu, X.; Weiss, R. A. *Macromolecules* **1992**, *25*, 3242−3246.
(22) Kwei, T. K. *J. Polym. Sci., Part C: Polym. Lett.* **1984**, *22*, 307−313.
(23) Kwei, T. K.; Pearce, E. M.; Pennacchia, J. R.; Charton, M. *Macromolecules* **1987**, *20*, 1174−1176.
(24) Kuo, S. W.; Chang, F. C. *Macromolecules* **2001**, *34*, 4089−4097.
(25) Purcell, K. F.; Drago, R. S. *J. Am. Chem. Soc.* **1967**, *89*, 2874−2880.
(26) Chen, C.-L. In *Springer series in wood science*; Dence, C. W., Ed.; Springer-Verlag: Berlin, New York, 1992; pp 301−321.
(27) Lin, S. Y. In *Methods in lignin chemistry*; Dence, C. W., Ed.; Springer-Verlag: Berlin, New York, 1992; pp 217−232.
(28) Lundquist, K. In *Methods in lignin chemistry*; Lin, S. Y., Dence, C. W., Eds.; Springer-Verlag: Berlin, New York, 1992; pp 242−249.
(29) Kubo, S.; Ishikawa, N.; Uraki, Y.; Sano, Y. *Mokuzai Gakkaishi* **1997**, *43*, 655−662.
(30) Hoffman, J. D.; Weeks, J. J. *J. Chem. Phys.* **1962**, *37*, 1723−1738.
(31) Li, Y.; Sarkanen, S. *Macromolecules* **2002**, *35*, 9707−9715.
(32) Guo, Q. P.; Huang, J. Y.; Li, B. Y.; Chen, T. L.; Zhang, H. F.; Feng, Z. L. *Polymer* **1991**, *32*, 58−65.
(33) Ikeda, T.; Holtman, K.; Kadla, J. F.; Chang, H. M.; Jameel, H. *J. Agric. Food Chem.* **2002**, *50*, 129−135.
(34) Wolf, M.; Wendorff, J. H. *Polym Commun* **1990**, *31*, 226−228.
(35) Lin, A. A.; Kwei, T. K.; Reiser, A. *Macromolecules* **1989**, *22*, 4112−4119.
(36) Brisson, J.; Breault, B. *Macromolecules* **1991**, *24*, 495−504.
(37) Nishi, T.; Wang, T. T.; Kwei, T. K. *Macromolecules* **1975**, *8*, 227−234.
(38) Cheung, Y. W.; Stein, R. S. *Macromolecules* **1994**, *27*, 2512−2519.
(39) Jonza, J. M.; Porter, R. S. *Macromolecules* **1986**, *19*, 1946−1951.
(40) Jo, W. H.; Lee, S. C. *Macromolecules* **1990**, *23*, 2261−2265.
(41) Iriarte, M.; Iribarren, J. I.; Etxeberria, A.; Iruin, J. J. *Polymer* **1989**, *30*, 1160−1165.


MA0348371